Heavy quark free energies and screening in SU(2) gauge theory

S. Digal and S. Fortunato
Fakultät für Physik, Universität Bielefeld, D-33501 Bielefeld, Germany

P. Petreczky
Nuclear Theory Group, Department of Physics, Brookhaven National Laboratory, Upton, New York 11973-500, USA
(Received 25 April 2003; published 12 August 2003)

We study the properties of the free energy of an infinitely heavy quark–antiquark pair in SU(2) gauge theory. By means of lattice Monte Carlo simulations we calculated the free energies in the singlet, triplet, and color averaged channels, both in the confinement and deconfinement phases. The singlet and triplet free energies are defined in the Coulomb gauge which is equivalent to their gauge invariant definitions recently introduced by Philipsen. We analyze the short and the long distance behavior, making comparisons with the zero temperature case. The temperature dependence of the electric screening mass is carefully investigated. The order of the deconfining transition is manifest in the results near T_c and it allows a reliable test of a recently proposed method to renormalize the Polyakov loop.

DOI: 10.1103/PhysRevD.68.034008 PACS number(s): 11.15.Ha, 11.10.Wx, 12.38.Mh, 25.75.Nq

I. INTRODUCTION

The study of the free energy of a static heavy-quark–antiquark pair in a medium of color charges at some temperature T has recently become a hot topic of statistical QCD [1–4]. The main reason is the fact that such free energy is related to the potential between quarks and antiquarks, which is of fundamental importance both for understanding deconfinement and in heavy quark phenomenology at finite temperature [5,6]. The study of static quark free energies (Polyakov loop correlators) is also important for constructing effective theories at the deconfinement transition [7].

The presence of the medium affects the quark–antiquark interaction in a nontrivial way. Such modifications of interactions are usually studied in terms of the free energy of a static quark–antiquark pair separated by some distance r. So far most studies concentrated on the behavior of the static quark–antiquark free energy at large distances, $r \gg 1/T$ [1,8,9]; below the deconfinement temperature T_c such behavior is characterized by a temperature dependent string tension, above T_c by exponential screening which is governed by a temperature dependent (Debye) screening mass. However, it turned out that the free energies of a static quark–antiquark pair exhibit a quite complex temperature behavior already at short distances $r < 1/T$ [3,10–12]. Furthermore, the detailed study of the free energy at short distances allows us to define a renormalized order parameter [3]. As far as the physics of heavy quarkonia is concerned, the detailed structure of the static quark–antiquark free energy at short distances is even more important than its large distance behavior. Though the large distance behavior of the color averaged potential was extensively studied in Refs. [1,8,9] the problem was not completely settled. This is partly due to finite size effects and very large statistics needed in such studies.

In this paper we want to study various features of the heavy-quark free energy in SU(2) gauge theory at finite temperature. The study of SU(2) lattice gauge theory has at least two advantages: the simulations are not so time consuming as in SU(3) and the deconfinement transition is second order, which has interesting consequences on the behavior of the free energy near the critical temperature T_c. In general, the heavy-quark free energy depends on the color channel one considers; for a complete analysis we investigated the singlet, the triplet, and the color averaged channels. In particular the study of the color singlet free energy is of interest because it is the most relevant quantity as far as the physics of heavy quarkonia at finite temperature is concerned. We examined both the short and the long-distance behavior of the free energies, below and above the deconfinement temperature. We devoted special attention to the issue of screening, in that we determined the Debye masses at various temperatures.

The rest of the paper is organized as follows. In Sec. II we define the free energy of a static quark–antiquark pair in color singlet, color triplet, and color averaged channels and discuss the choice of the simulation parameters. The basic features of the static quark–antiquark free energies are also discussed there. In Sec. III we present the numerical results below T_c. Section IV deals with free energies above deconfinement and determination of the screening masses. In Sec. V we define the renormalized Polyakov loop for SU(2) gauge theory following Ref. [3]. Finally Sec. VI contains our conclusions.

II. FREE ENERGIES IN SU(2) GAUGE THEORY

On the lattice the free energy of a static quark–antiquark pair in the gluonic medium is determined by correlation functions of temporal Wilson lines L,

$$L(\vec{r}) = \prod_{\tau=0}^{N_\tau - 1} U_0(\vec{r}, \tau), \tag{1}$$

$\mathrm{Tr}\, L$ is also referred to as the Polyakov loop. Following Refs. [13,14] we introduce the color singlet and triplet free energy of a static quark–antiquark pair

$$e^{-F_1(r,T)/T+C}=\frac{1}{2}\langle \mathrm{Tr}[L(\vec{r})L^\dagger(\vec{0})]\rangle, \tag{2}$$

$$e^{-F_3(r,T)/T+C}=\frac{1}{3}\langle \mathrm{Tr}\,L(\vec{r})\mathrm{Tr}\,L^\dagger(\vec{0})\rangle-\frac{1}{6}\langle \mathrm{Tr}\,L(\vec{r})L^\dagger(\vec{0})\rangle \tag{3}$$

as well as the color averaged free energy defined by

$$e^{-F_{\mathrm{avg}}(r,T)/T+C}=\frac{1}{4}\langle \mathrm{Tr}\,L(\vec{r})\mathrm{Tr}\,L^\dagger(\vec{0})\rangle. \tag{4}$$

The latter can be written as a thermal average of the free energies in singlet and triplet channels, hence the name,

$$e^{-F_{\mathrm{avg}}(r,T)/T}=\frac{1}{4}e^{-F_1(r,T)/T}+\frac{3}{4}e^{-F_3(r,T)/T}. \tag{5}$$

The normalization constant C can be defined in different ways. In the deconfined phase it is customary to set $C=\ln|\langle\frac{1}{2}\mathrm{Tr}\,L\rangle|^2$. Another possibility is to fix it by normalizing the singlet free energy to the zero temperature heavy quark potential [3].

The main problem with the definitions of the singlet and triplet free energies (2), (3) is that these definitions are not gauge invariant, as the Wilson line is not a gauge invariant quantity. The only manifestly gauge invariant quantity is the color averaged free energy. This is the reason why singlet and triplet free energies were not studied in much detail so far. It was recently shown by Philipsen that gauge invariant definitions of the singlet and triplet free energies can be achieved by replacing the Wilson line in Eqs. (2), (3) by a gauge invariant Wilson line defined by

$$\tilde{L}(\vec{r})=\Omega^\dagger(\vec{r})L(\vec{r})\Omega(\vec{r}). \tag{6}$$

The SU(2) matrix $\Omega(\vec{R})$ is constructed from eigenvectors of the spatial covariant Laplacian (see Ref. [2] for further details). Furthermore, it was shown that this definition is equivalent to the definitions of the singlet and triplet free energies in Coulomb gauge. Since the determination of eigenvectors of the covariant Laplacian is computationally very expensive we fix the Coulomb gauge to calculate the singlet and triplet free energies.

In our numerical investigations we use the standard Wilson action. In order to get control over finite size effects, which become important in the vicinity of T_c, we have performed simulations at several different volumes. As we also want to investigate the short distance behavior of the free energies, simulations were performed for $N_\tau=4,6,8$. To fix the temperature scale we have used the nonperturbative beta function of Ref. [15]. We will also use $T_c/\sqrt{\sigma}=0.69$ [16], with σ being the zero temperature string tension. The lattice volumes and the gauge coupling along with the corresponding temperatures used in our simulations are summarized in Table I.

Calculations of the zero temperature potential and of the free energy of the static quark–antiquark pair show lattice artifacts, e.g., violation of rotational symmetry at short distances. Since we are also interested in the behavior of the potential at short distances, we should try to remove these lattice artifacts. At short distances it is expected that the dominant contribution to the potential is given by one-gluon exchange and thus it is natural to start the discussion of the cutoff effects in the Coulomb potential calculated on the lattice. The lattice Coulomb potential is given by

$$C_L(r)=\int\frac{d^3k}{(2\pi)^3}\exp(i\vec{k}\cdot\vec{r})\frac{1}{4a^{-2}\sum_{i=1,3}\sin^2(k_ia/2)}, \tag{7}$$

with a being the lattice spacing. In the limit $a\to 0$, $\sin^2 k_ia/2\simeq\vec{k}^2a^2/4$ and the usual continuum Coulomb potential is recovered. However, one can easily see that keeping the second term in the expansion of $\sin k_ia/2$ will lead to the appearance of terms of order a^2/r^3, which in turn will depend not only on the value of r but also on whether the separation vector $\vec{r}$ lies on the coordinate axis or is aligned along other possible directions, indicating the breakdown of rotational symmetry. Following Ref. [17] we replace $F_i(r)$ by $F_i(r_I)$ where $r_I=[4\pi C_L(r)]^{-1}$. In this way we replace the lattice separation by the separation r_I which corrects for the tree level artifacts in the Coulomb potential calculated on the lattice. When presenting the data on the free energy we will always do this replacement unless stated otherwise.

Let us now present some general features of our findings. First we have performed simulations at a fixed lattice spacing, corresponding to the gauge coupling $\beta=2.5$ at $N_\tau=12$ and 6 corresponding to temperatures $T=0.6T_c$ and $1.3T_c$, respectively. The results are shown in Fig. 1 (left). At this value of the gauge coupling the ground state static quark–antiquark potential as well as the first two excited potentials at $T=0$ have been calculated [18] and we show them in Fig. 1 together with our data. The singlet free energies at short distances do not differ from the zero temperature potential and temperature dependence shows up only at $r\sqrt{\sigma}>0.5$. The triplet free energy and the triplet potential at $T=0$ were not studied in detail so far beyond perturbation theory. At zero temperature it was shown that the excited potential coincides with the triplet potential at very short distances up to a nonperturbative constant [19]. This is also supported by lattice calculations in SU(3) gauge theory (there one has to talk about the octet potential of course) [21]. We expect that our definition of the triplet free energy should match smoothly the perturbative zero temperature triplet potential at very short distances without any constant, in the same way as the singlet free energy approaches the singlet zero temperature potential. This is the reason why the triplet free energy is smaller than the excited potential as shown in Fig. 1. We find that the triplet free energy is temperature independent at short distances.

In most of our calculations we have varied the temperature T by varying the lattice spacing a (i.e., the gauge coupling $\beta=4/g^2$) for fixed temporal extent N_τ. As both the free energy and the $T=0$ potential contain a lattice spacing dependent additive constant C [cf. Eqs. (2)–(5)], some normalization prescription should be introduced in order to

TABLE I. Lattice volumes and gauge couplings $\beta=4/g^2$ used in our simulations. The values of T/T_c were obtained using the nonperturbative beta function [15].

$N_\tau=4$			$N_\tau=6$			$N_\tau=8$			$N_\tau=12$		
β	T/T_c	N_σ	β	T/T_c	N_σ	β	T/T_c	N_σ	β	T/T_c	N_σ
2.1962	0.70	32	2.5000	1.30	32	2.4781	0.90	32	2.5000	0.60	32
2.2340	0.80	16,32				2.7385	2.00	32			
2.2681	0.90	16,32				2.8765	3.00	32			
2.2745	0.92	32,60				3.1228	6.062	32			
2.2807	0.94	32				3.2218	8.00	32			
2.2838	0.95	32,60				3.3680	12.00	32			
2.2900	0.97	32,60									
2.2930	0.98	60									
2.2960	0.99	32,60									
2.2975	0.995	32									
2.3019	1.01	32,48,60									
2.3077	1.03	32									
2.3134	1.05	16,32,48									
2.3272	1.10	32									
2.3533	1.20	16,32									
2.3776	1.30	32									
2.4215	1.50	16,32									
2.5118	2.00	16,32									
2.6431	3.00	32									
2.8800	6.062	32									
2.9766	8.000	32									
3.0230	9.143	32									
3.2190	15.87	16									

compare the free energies calculated at different temperatures. To do so we assume the following form for the zero temperature potential:

$$V(r)/\sqrt{\sigma}=-\frac{0.238}{r\sqrt{\sigma}}+r\sqrt{\sigma}+\frac{0.0031}{(r\sqrt{\sigma})^2}. \tag{8}$$

This form was obtained in Ref. [20] by fitting the lattice data on the $T=0$ potential for $r\sqrt{\sigma}>0.063$ at $\beta=2.85$ apart from the constant which we have omitted. The violation of rotational invariance on the lattice was taken into account in the fit procedure. Thus Eq. (8) defines our convention for the continuum zero temperature potential. In some cases we

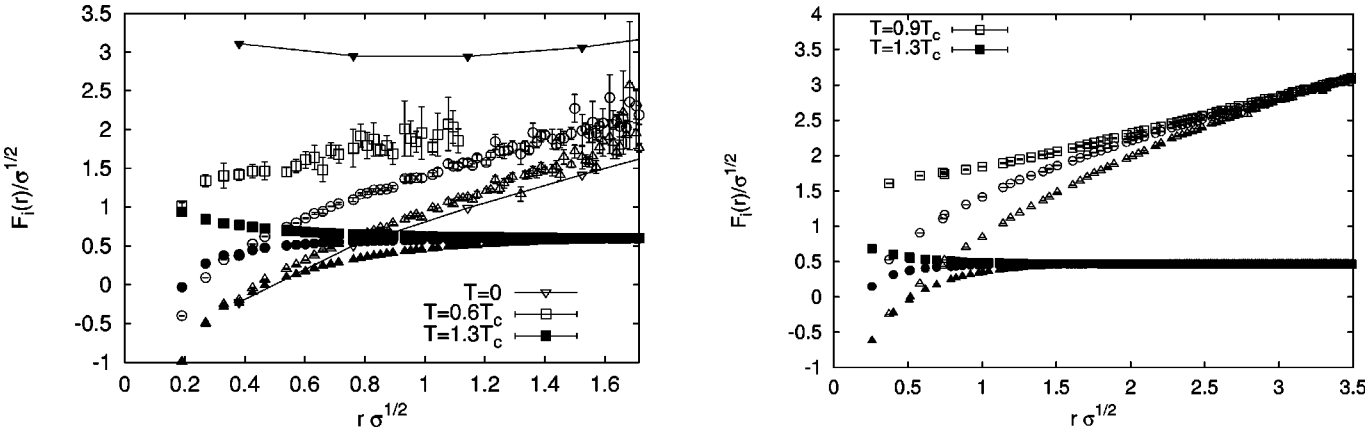

FIG. 1. (Left) Free energies of a static quark–antiquark pair as a function of the distance $r\sqrt{\sigma}$ at $T=0.6T_c$ (open symbols) and $T=1.3T_c$ (closed symbols) corresponding to coupling $\beta=2.5$. Also shown is the $T=0$ potential and its first excitation (open and closed lower triangles correspondingly connected by lines) at the same β value. (Right) The free energies are here calculated at $N_\tau=4$; the temperature values are $T=0.9T_c$ and $1.3T_c$, respectively. The triangles, squares, and circles indicate the singlet, the triplet, and the averaged free energies, respectively.

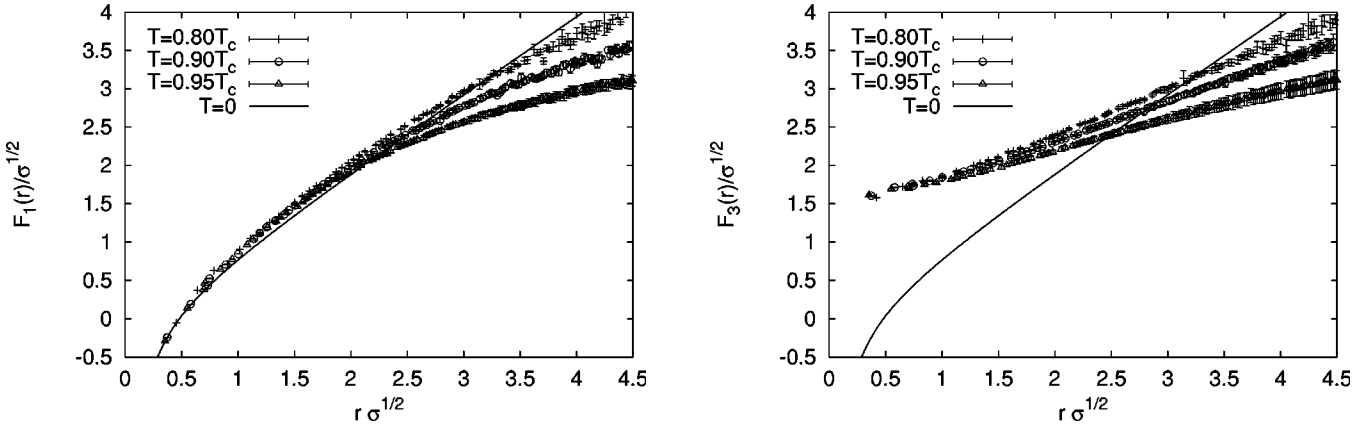

FIG. 2. The color singlet (left) and triplet (right) free energies at various temperatures in the confinement phase calculated for $N_\tau=4$. The normalization constant C was chosen such that the singlet free energy matches the zero temperature potential (solid line) at the shortest distance (see text).

need the $T=0$ potential at distances $r\sqrt{\sigma}<0.063$. In this case we use the three-loop perturbative potential calculated in the qq scheme [22] normalized to smoothly match the form defined by Eq. (8) at $r\sqrt{\sigma}=0.07$. We have also checked that the difference between the three-loop and two-loop results is negligible for our purposes. In what follows the normalization constant C will be chosen such (unless stated otherwise) that the singlet free energy matches the $T=0$ potential at the shortest distance $(r/a=1)$. In Fig. 1 (right) we show our results on static free energies calculated for $N_\tau=4$ and using this normalization convention. The free energies in the deconfined phase reach the same value at large distances (see Fig. 1). This is to be expected as at very large distances due to screening the free energy of color charges should be independent of their relative color orientation.

III. RESULTS IN THE CONFINEMENT PHASE

In this section we are going to present our numerical results in the confinement phase. In Fig. 2 we show the singlet and triplet free energies with the normalization described in the previous section. One can see that the temperature dependence of the singlet free energy is only visible at distances $r\sqrt{\sigma}>2$. The triplet free energy is also temperature independent at small distances; thermal effects become visible at $r\sqrt{\sigma}>1.4$. We also notice that there is a slight enhancement of the singlet free energy over the $T=0$ potential in the interval $1<r\sqrt{\sigma}<2$. A similar enhancement was observed also in the case of $(2+1)$-dimensional SU(2) gauge theory at finite temperature [2] as well as in preliminary SU(3) calculations [4]. As the color averaged free energy is a thermal average of singlet and triplet free energies, it would have a nontrivial temperature dependence even if the latter were temperature independent. This temperature dependence is larger the smaller the gap between the triplet and singlet contributions. In general one can say that the temperature dependence of the color averaged free energy at short and intermediate distances is mostly determined by the value and the temperature dependence of the color triplet contribution. If this continues to be true in full QCD, then some of the conclusions of Ref. [6] (where the color averaged free energy was related to the meson masses) should be revised.

At large distances the color singlet, triplet, and averaged free energy reach a common value which can be parametrized by a form

$$F_i(r,T)\big|_{rT\gg 1}=\sigma(T)r+A(T)\ln rT+B(T). \qquad (9)$$

In Fig. 3 we show the color averaged free energy as well as the string tension obtained from it using the fit to Eq. (9). Because the deconfinement transition is of second order, the inverse correlation length (string tension) vanishes at T_c. As a result we have large finite size effects close to T_c. Indeed we found that on the $32^3\times 4$ lattice the string tension vanishes around $0.97T_c$. For this reason we performed simulations on the larger $60^3\times 4$ lattice close to T_c. We have seen that the values of $\sigma(T)$ we have obtained from our calculations on $32^3\times 4$ lattice agree with the results from the $60^3\times 4$ lattice up to $0.92T_c$. Above such temperature we adopt the results from the larger lattice. The final situation is illustrated in Fig. 3 (right), where the squares indicate the results from $60^3\times 4$, the crosses the ones from $32^3\times 4$. It is well known that $\sigma(T)$ vanishes near T_c according to the power law $\sigma(T)\propto(T_c-T)^\nu$, where $\nu=0.63$ is the 3D Ising exponent for the correlation length. Therefore we tried to fit our data point by using the ansatz $\sigma(T)=a(T_c-T)^\nu[1+b(T_c-T)^{1/2}]$, with $\nu=0.63$. The best fit curve is shown in our plot and it reproduces very well our data. The values of $\sigma(T)$ found by us are considerably smaller than those obtained in Ref. [8]. This is probably due to the fact that the lattice volumes used in Ref. [8] were considerably smaller than ours.

IV. RESULTS IN THE DECONFINEMENT PHASE: SCREENING

We start our discussion of the numerical results in the deconfined phase with Fig. 4, where we show the singlet free energy in units of $\sqrt{\sigma}$ normalized to the zero temperature potential at the shortest distance. As one can see the singlet free energy saturates at large distances, while at short enough

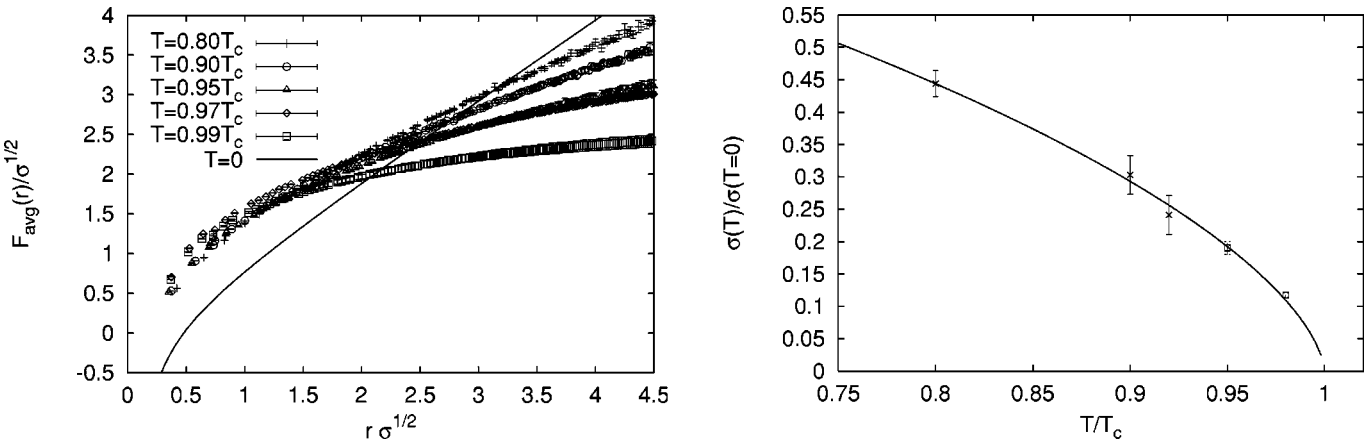

FIG. 3. (Left) Color averaged free energies at various temperatures in the confinement phase. (Right) String tension as a function of T/T_c, crosses correspond to a $32^3\times4$ lattice, open squares to a $60^3\times4$ lattice.

distances it is temperature independent and coincides with the zero temperature potential. The distance in physical units, at which the temperature dependence enters, of course strongly depends on the value of the temperature, the higher the temperature the shorter is the distance where effects of the medium become visible. Also the distance where the singlet free energy saturates strongly depends on the temperature, it is getting larger as we approach T_c. Close to T_c screening enters only at distances $r\sqrt{\sigma}>1$. This feature of the free energy is reflected in the temperature dependence of the screening masses which will be discussed below. Another interesting feature of the singlet free energy is that the value of the plateau of the free energy decreases with the temperature. Such a behavior of the singlet free energy was observed for SU(3) gauge theory in Ref. [3], where it was also argued that the reason for this is the presence of the entropy contribution.

For the further discussion of the results in the deconfined phase, especially for making comparisons with perturbation theory, it is more convenient and in fact customary (cf. [1,11]) to choose the renormalization constant C in Eqs. (2), (3) to be $C=\ln|\langle\frac{1}{2}\mathrm{Tr}\,L\rangle|^2$. Furthermore, the large distance behavior of the free energies should be discussed separately from their short distance behavior, where one would expect perturbation theory to work. In general it is expected that perturbation theory breaks down at distances $r>1/g^2T$ [24], with g being the gauge coupling constant. As for the physically interesting temperature range one always has $g\sim1$, perturbation theory may be applicable at distances $rT<1$. One of the predictions of perturbation theory is that $-3F_3(r,T)/F_1(r,T)\simeq1$, for any r. In Fig. 5 we show this ratio for different temperatures. This ratio appears indeed to be constant for $T>1.5T_c$ but always smaller than 1, even for the highest temperature we considered $(16T_c)$. Similar results were found in Landau gauge in Refs. [10,23].

High temperature perturbation theory at leading order predicts that the color averaged free energy has the form [13,25]

$$\frac{F_{\mathrm{avg}}(r,T)}{T}=-\frac{3}{32}\frac{g^4}{(4\pi rT)^2}e^{-2m_{D0}r} \tag{10}$$

at distances $r>1/T$, with m_{D0} being the leading order Debye mass $m_{D0}=\sqrt{2/3}gT$. At distances $r<1/T$ the simple form (10) is no longer valid, though the $1/r^2$-like behavior is still expected due to cancellation between singlet and triplet con-

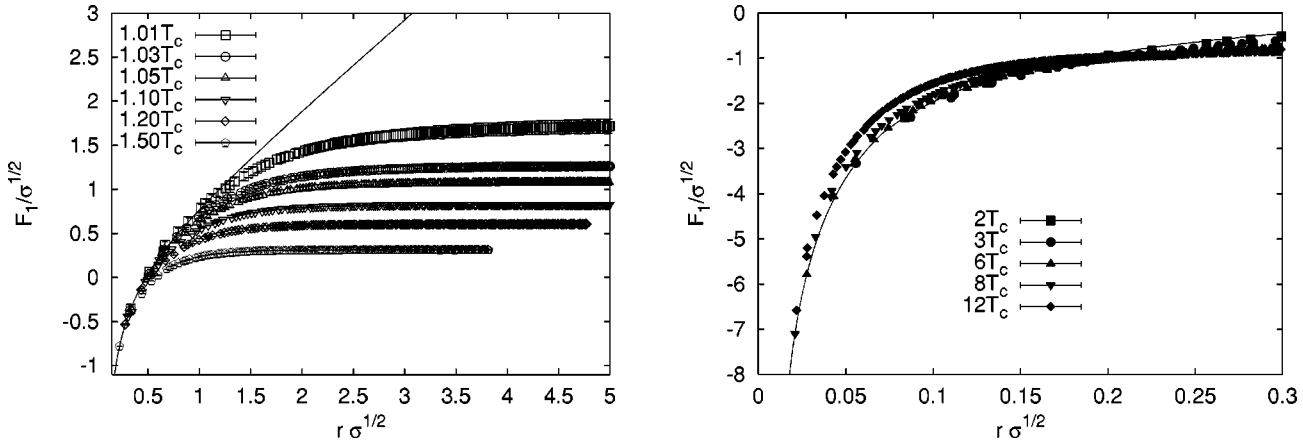

FIG. 4. The color singlet free energy at various temperatures in the deconfinement phase calculated for $N_\tau=4$ (left) and $N_\tau=8$ (right). The solid line is the $T=0$ potential.

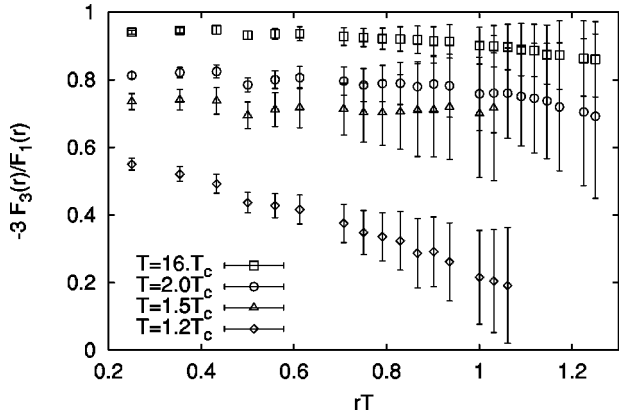

FIG. 5. Free energy triplet/singlet ratio at various temperatures.

tributions [13]. Therefore we define the so-called screening function $S(r,T)$ by the formula

$$\frac{F_{\rm avg}(r,T)}{T} = -\frac{3}{32}\frac{1}{(rT)^2}S(r,T). \tag{11}$$

In Fig. 6 we show the numerical results for the square root screening function. As one can see from the figure, at high temperatures ($T>2T_c$) the screening function shows a mild r-dependence, which implies that the color averaged free energy behaves like $1/r^2$. The screening function $S(r,T)$ decreases with increasing temperature which one would expect if $S(r,T)\sim g^4(T)$. At temperatures closer to T_c the screening function decreases at small distances. Obviously, this behavior has nothing to do with screening and signals the breakdown of the high temperature expansion. As we approach T_c $F_{1,3}/T$ is no longer small at small distances as shown in Fig. 6 and therefore the exponentials in Eq. (5) cannot be expanded. As a result of this, the cancellation between the singlet and triplet free energies no longer holds; moreover, since the singlet free energy is negative and the triplet one is positive (when working with normalization convention $C=\ln|\langle\frac{1}{2}\,\mathrm{Tr}\,L\rangle|^2$) the color averaged free energy is dominated by the singlet contribution and behaves like $1/r$ at small distances. We also note that the free energies calculated for different N_τ (different lattice spacing) at $3T_c$ agree reasonably well. Similar agreement between the results calculated for different values of N_τ was observed for other temperatures too.

Let us now discuss the large distance behavior of the free energies and the determination of the screening masses. We will restrict ourselves to the discussion of the color singlet and color averaged free energy as the color triplet free energy becomes very noisy at large distances and the present statistics do not allow one to study it in detail.

Contrary to earlier studies [1,8,11], where the screening masses were obtained using uncorrelated fit and the short and large distance behaviors of the free energy were not separated from each other, here we use the correlated fit procedure of Ref. [26]. From Fig. 6 it is clear that in the region $rT<1$ the color averaged free energy can be well described by almost unscreened $1/r^2$-like behavior. Therefore this region should not be considered for the determination of the screening masses. In our procedure the fit interval was chosen so that the fit yields a reasonable $\chi^2/[\text{No. degree of freedom (DOF)}]$. Thus, unlike in the uncorrelated fit used in Ref. [1], there is no dependence of the screening masses on the fit interval. We determine the screening mass in the color singlet channel by fitting the data with a screened Coulomb (Yukawa-like) ansatz. In leading order perturbation theory, in fact, the most important contribution to the singlet free energy is given by the exchange of a single gluon. In the case of the color average free energy we used a more general fit ansatz [27]:

$$\frac{F_{\rm avg}}{T} = \frac{A}{r^d}\exp(-\mu R) + B. \tag{12}$$

As possible values for the exponent d we took $d=1,2$. The resulting values of the screening masses that we extracted are presented in Tables II and III for the singlet and the averaged channels, respectively. For determination of the screening masses we mostly use a $32^3\times 4$ lattice.

We found that for the color averaged free energy the fits with $d=1$ and $d=2$ are both good for all temperatures, except near T_c, where we got a reasonable $\chi^2/(\text{No. DOF})$ only for $d=1$. From our fit analysis it then comes out that we

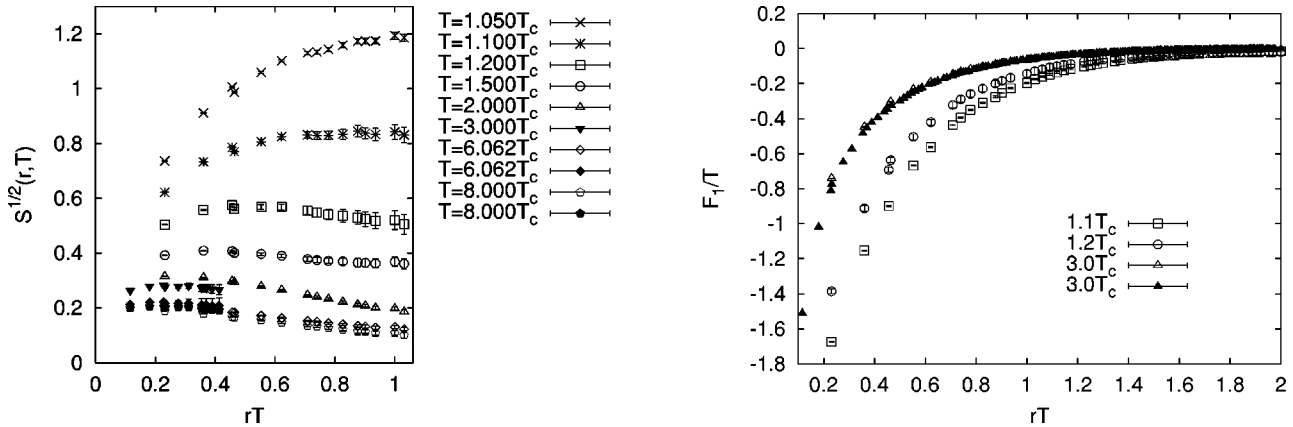

FIG. 6. The square root of the screening function (left) and the singlet free energy in units of T (right) at different temperatures. The open symbols refer to the results for $N_\tau=4$, the closed symbols to the results for $N_\tau=8$.

TABLE II. Screening masses extracted from color singlet free energy.

Color singlet correlators		
β	T/T_c	$\mu_e(T)/T$
2.3019	1.01	0.884(80)
2.3077	1.03	1.356(52)
2.3134	1.05	1.75(10)
2.3272	1.10	2.23(4)
2.3533	1.20	2.35(24)
2.3776	1.30	2.50(6)
2.4215	1.50	2.62(6)
2.5118	2.00	2.37(9)
2.8800	6.062	1.912(44)
3.0230	9.143	1.812(36)

cannot choose between the two cases, which gives a systematic error of about 30% on the screening masses. In order to eliminate this ambiguity, we have also calculated the plane-plane correlator, given by the formula:

$$C_{PL}(x_3)=\langle \mathrm{Tr}L(x_3)\mathrm{Tr}\,L^{\dagger}(0)\rangle-|\langle \mathrm{Tr}\,L\rangle|^2, \qquad (13)$$

where $L(x_3)\equiv\Sigma_{x_1,x_2}L(x_1,x_2,x_3)$. If the color averaged free energy has the form (12) with $d=1$, then $C_{PL}(x_3)$ should fall off with the distance as a simple exponential, which allows a direct determination of the screening mass. The results we found are reported for comparison in Table III. We see that the values of the masses extracted from the plane-plane correlator agree in each case with the masses obtained from the point-point correlator when $d=1$. Furthermore, we have analyzed the effective masses extracted from $C_{PL}(x_3)$. They reach a plateau already at $x_3T\sim 1$, which makes the presence of power-like prefactors in $C_{PL}(x_3)$ at large distances very unlikely and thus implying that very likely $d\simeq 1$. At high temperature dimensional reduction arguments suggest that $d=1$, as the large distance behavior of any static correlators is governed by exchange of a bound state of the effective three-dimensional theory [28].

TABLE III. Screening masses extracted from color averaged free energy and from plane-plane correlators of Polyakov loops (see text).

Color averaged correlators				
		$\mu_{\mathrm{avg}}(T)/T$, extracted from		
β	T/T_c	Point-C, d=1	Point-C, d=2	Plane-C
2.3019	1.01	0.424(20)	<0	0.468(28)
2.3134	1.05	1.000(28)	0.544(20)	1.024(16)
2.3533	1.20	1.95(13)	1.19(22)	1.93(6)
2.3776	1.30	2.31(16)	1.332(88)	2.296(64)
2.5112	2.00	2.69(15)	2.06(12)	2.89(18)
2.8800	6.062	3.03(10)	2.32(10)	
3.0230	9.143	3.04(20)	2.04(56)	

For $T=1.01T_c$ the results refer to the $48^3\times 4$ lattice instead of $32^3\times 4$. In this case, in fact, the mass changes appreciably when one goes to the larger $48^3\times 4$ lattice. This is probably due to the large correlation length close to T_c. Further simulations on a $60^3\times 4$ lead to the same value of the mass we found on the $48^3\times 4$, which is then reliable as infinite volume limit at this temperature.

In Fig. 7 we show the screening masses extracted from the singlet free energy as a function of the temperature. There we also show the values of the screening masses obtained from the electric gluon propagator in Landau gauge [23,29] at $T>1.2T_c$. As one can see they are compatible with the singlet masses we have found. This is to be expected in perturbation theory. It was shown, however, by Nadkarni that this is true in general at large distances $r\gg 1/T$ [14]. In Fig. 7 the color averaged screening masses are shown as well; we compared them with the lowest A_1^+ scalar screening mass (spatial glueball mass) obtained in Ref. [30]. Dimensional reduction arguments [28] suggest that these masses should agree at high temperature and the figure seems to indicate that this is indeed the case. Very recently the plane-plane correlators of Polyakov loops were studied in Ref. [31] for $T=1.1105T_c$ and $1.227T_c$ (we use the nonperturbative beta function [15] to convert the gauge coupling of Ref. [31] to temperature). In Fig. 7 we show as well the corresponding screening masses (open triangles). Moreover, we note that the color averaged screening masses obtained by us using fits with $d=2$ agree with the findings of Refs. [9,32] where the same exponent was used. The color averaged screening mass should go to zero when $T\to T_c$ because it is just the inverse of the Polyakov loop correlation length, which diverges at T_c. On the other hand there is no *a priori* argument for which the singlet mass should vanish at the threshold. Figure 7 indicates that both masses become very small near T_c.

V. THE RENORMALIZED POLYAKOV LOOP

The last issue we would like to address is the renormalization of the Polyakov loop. It is known that if one takes the continuum limit at fixed temperature, the expectation value of the Polyakov loop vanishes, so that the usual definition does not really provide a physical order parameter for deconfinement. As we have already said at the beginning, the free energies on the lattice are always defined up to some renormalization constant. According to a recent work [3], a suitable choice of such a renormalization constant can lead to a new definition of the Polyakov loop. If the constant is chosen such that the singlet free energy matches the zero temperature heavy quark potential at short distances, one can define a ''renormalized'' Polyakov loop L_{ren} through the formula:

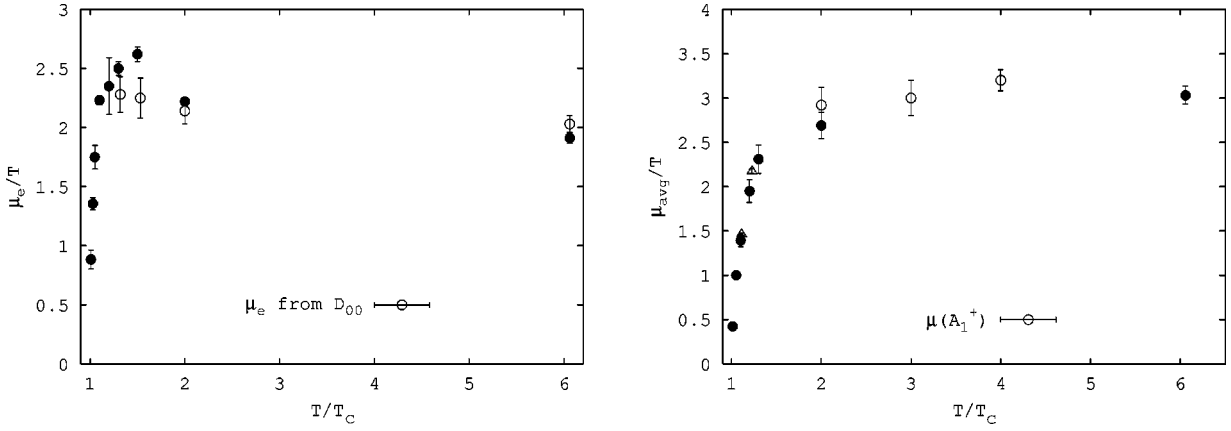

FIG. 7. Screening masses in units of temperature vs T/T_c extracted from the color singlet free energy (left) and from the color averaged free energy (right). In the left plot we have also shown the screening mass extracted from the static electric propagator [23,29]. In the right plot we give the lowest A_1^+ screening mass from [30] as well as the screening masses of plane-plane correlators of Polyakov loops from [31] (open triangles).

$$L_{\rm ren} = \exp[-F_\infty(T)/2T], \tag{14}$$

where $F_\infty(T)$ is the asymptotic value of the singlet free energy at the temperature T (in fact, it does not depend on relative color orientation of the quark–antiquark pair, see above). We remind the reader that we have renormalized the singlet free energy exactly in this way, so that, in our case, $F_\infty(T)$ is nothing but the height of the plateau of the curves in Fig. 4. Practically we took $F_\infty(T) = F_1(N_\sigma/2, T)$, which is the value of the free energy at the largest distance allowed on the lattice. In Fig. 8 we plot the renormalized Polyakov loop as function of the temperatures. When normalizing the singlet free energy to the $T=0$ potential at the shortest distance $(r/a=1)$ we implicitly assume that there is no temperature dependence at this distance. This may not always be the case. Therefore we also calculate $F_\infty(T)$ and the corresponding $L_{\rm ren}$ by normalizing the singlet free energy to the $T=0$ potential as well as at $r/a=\sqrt{2}$. The difference in $F_\infty(T)$ $(L_{\rm ren})$ arising from these two normalizations gives us an estimate of possible systematic errors. When quoting the error on the renormalized Polyakov loop we always add quadratically the systematic and the statistical errors. At variance with SU(3), we now have a second order phase transition and a well defined scaling behavior of $L_{\rm ren}$ at criticality. In order to check the scaling we have fitted the data on $L_{\rm ren}$ using the standard ansatz in the interval $T_c < T \leqslant 1.5 T_c$,

$$L_{\rm ren}(T) = c(T-T_c)^\beta [1 + b(T-T_c)^\omega], \tag{15}$$

with the exponents β and ω fixed to their SU(2) values $\beta = 0.3265$ and $\omega = 1$. The fit curve is shown in Fig. 8 (dashed line) and reproduces quite well the pattern of the data points. We have also performed fits setting $b=0$ and considering temperatures $T \leqslant 1.1 T_c$. This fit gives similar values of c as the fits with $b \neq 0$ discussed above.

VI. CONCLUSIONS

In conclusion we have studied the quark–antiquark free energies in SU(2) gauge theory below and above the deconfinement temperature. We have found that the temperature dependence of the singlet free energy is much weaker than the temperature dependence of the color averaged free energy. Most of the temperature dependence of the color aver-

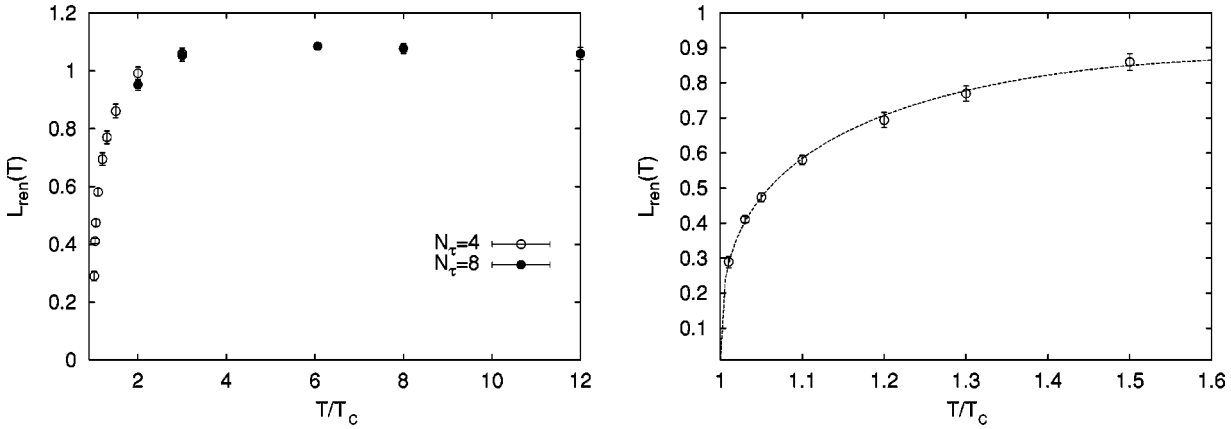

FIG. 8. Renormalized Polyakov loop as a function of the temperature in the entire temperature interval (left) and for $T \leqslant 1.5 T_c$ together with the fit (right). The error bars indicate the combined statistical and systematic errors.

aged free energy is due to the presence of the color triplet contribution and its temperature dependence. If this will hold for real QCD it may have important consequences in the heavy quarkonia phenomenology at finite temperature. At large distances the free energy in color singlet and triplet channels converge to a common value.

Above T_c the color singlet free energy can be understood in terms of propagation of a nonperturbatively screened gluon. Through the detailed analysis of the point-point and plane-plane correlators as well as comparisons with other determinations of the screening masses, we have established that the color averaged free energy is described by Yukawa law at large distances, whereas at shorter distances it exhibits a more complex behavior. At low temperatures and short distances the color averaged free energy is dominated by the singlet contribution, while at higher temperatures it has $1/r^2T$ behavior and its temperature dependence is qualitatively the same as predicted by perturbation theory. Finally we have shown that the renormalized Polyakov loop defined in [3] has the correct scaling behavior near the critical temperature.

As an outlook we note that we have studied the free energy of static charges in the fundamental representation. It will be interesting to investigate the free energy of static charges in other representations. Some work in this direction was done in [33].

ACKNOWLEDGMENTS

It is a pleasure to thank J. Engels, O. Kaczmarek, and F. Karsch for helpful discussions. We are grateful to A. Cucchieri, who provided us the gauge fixing routine. We would also like to thank the TMR network ERBFMRX-CT-970122 and the DFG Forschergruppe fFOR 339/2-1 or financial support. This work was partly supported by the U.S. Department of energy under Contract DE-AC02-98CH10886.

[1] O. Kaczmarek *et al.*, Phys. Rev. D **62**, 034021 (2000).
[2] O. Philipsen, Phys. Lett. B **535**, 138 (2002).
[3] O. Kaczmarek, F. Karsch, P. Petreczky, and F. Zantow, Phys. Lett. B **543**, 41 (2002).
[4] F. Zantow, O. Kaczmarek, F. Karsch, and P. Petreczky, hep-lat/0301015.
[5] T. Matsui and H. Satz, Phys. Lett. B **178**, 416 (1986).
[6] S. Digal, P. Petreczky, and H. Satz, Phys. Lett. B **514**, 57 (2001); Phys. Rev. D **64**, 094015 (2001).
[7] For a recent discussion and further references see: R.D. Pisarski, hep-ph/0203271.
[8] J. Engels *et al.*, Nucl. Phys. **B280**, 577 (1987).
[9] A. Irbäck *et al.*, Nucl. Phys. **B363**, 34 (1991).
[10] N. Attig *et al.*, Phys. Lett. B **209**, 65 (1988).
[11] J. Engels, F. Karsch, and H. Satz, Nucl. Phys. **B315**, 419 (1989).
[12] P. Petreczky *et al.*, Nucl. Phys. **A698**, 400 (2002).
[13] L.D. McLerran and B. Svetitsky, Phys. Rev. D **24**, 450 (1981).
[14] S. Nadkarni, Phys. Rev. D **34**, 3904 (1986).
[15] J. Engels, F. Karsch, and K. Redlich, Nucl. Phys. **B435**, 295 (1995).
[16] J. Fingberg, U.M. Heller, and F. Karsch, Nucl. Phys. **B392**, 493 (1992).
[17] S. Necco and R. Sommer, Nucl. Phys. **B622**, 328 (2002).
[18] C. Michael and S.J. Perantonis, J. Phys. G **18**, 1725 (1992).
[19] N. Brambilla, A. Pineda, J. Soto, and A. Vairo, Nucl. Phys. **B566**, 275 (2000).
[20] S.P. Booth *et al.*, Nucl. Phys. **B394**, 509 (1993).
[21] K.J. Juge, J. Kuti, and C. Morningstar, Proceedings of the John Hopkins Workshop on Current Problems in Particle Theory 24, Non-Perturbative QFT Methods and their Applications, Budapest, 2000, pp. 143–167, hep-lat/0103008.
[22] S. Necco and R. Sommer, Phys. Lett. B **523**, 135 (2001).
[23] U.M. Heller, F. Karsch, and J. Rank, Phys. Rev. D **57**, 1438 (1998).
[24] A.D. Linde, Phys. Lett. **96B**, 289 (1980).
[25] S. Nadkarni, Phys. Rev. D **33**, 3738 (1986).
[26] C. Michael and A. McKerrell, Phys. Rev. D **51**, 3745 (1995).
[27] In fact, in order to do the correlated fit we consider the connected correlators of Wilson lines, i.e., we subtract $|\langle \mathrm{Tr}\, L\rangle|^2$ from the correlator. As far as we are interested only in the large distance behavior this is equivalent to fitting the free energies. Only in the thermodynamic limit the connected correlator vanishes at very large distance. Therefore we allow for a constant B in our fit ansatz. It turns out, however, that this constant is compatible with zero within present statistical accuracy.
[28] K. Kajantie, M. Laine, K. Rummukainen, and M. Shaposhnikov, Nucl. Phys. **B503**, 357 (1997); F. Karsch, M. Oevers, and P. Petreczky, Phys. Lett. B **442**, 291 (1998); A. Hart and O. Philipsen, Nucl. Phys. **B572**, 243 (2000); A. Hart, M. Laine, and O. Philipsen, *ibid.* **B586**, 443 (2000); O. Philipsen, Nucl. Phys. (Proc. Suppl.) **94**, 49 (2001).
[29] U.M. Heller, F. Karsch, and J. Rank, Phys. Lett. B **355**, 511 (1995).
[30] S. Datta and S. Gupta, Nucl. Phys. **B534**, 393 (1998); Phys. Lett. B **471**, 382 (2000).
[31] R. Fiore, A. Papa, and P. Provero, Phys. Rev. D **67**, 114508 (2003).
[32] P. Lacock and T. Reisz, Nucl. Phys. B (Proc. Suppl.) **30**, 307 (1993).
[33] K. Redlich and H. Satz, Phys. Lett. B **208**, 291 (1988); **213**, 191 (1988).